A turbulence model for polymer flows

By Y. Dubief, G. Iaccarino AND S. K. Lele

1. Motivation and background

Recent advancements in the modeling of polymer drag reduction in the context of RANS simulation are discussed. The present model is derived from the current understanding of the mechanism of near-wall turbulence in drag reduced polymer flows described in Dubief *et al.* (2004) and adapted to the $v^2 - f$ turbulence model introduced by Durbin (1995) for Newtonian flows. Results for channel flows with homogeneous polymer concentrations prove to be very satisfactory. The model captures accurately the behavior of the mean velocity profiles for the two main regimes, called LDR and HDR, Low and High Drag Reduction, respectively.

1.1. *LDR and HDR*

For drag-reduced flows with polymers, turbulent statistics have been extensively characterized by experiments. Warholic *et al.* (1999) established the existence of two distinct statistical regimes. For a given polymer molecule, the mean velocity profile experiences an upward shift of its log-law region for the smallest concentration, up to a drag reduction (DR) of the order of 40%. This regime is referred to as the Low-Drag Reduction (LDR) regime. A further increase in concentration leads to a change in the slope of the log-law which defines the High-Drag Reduction (HDR) regime. As more polymers are added, the flow tends toward an asymptotic state, called the Maximum Drag Reduction (MDR) regime, for which drag is slightly higher than the laminar state Virk & Mickley (1970). The components of the Reynolds stress tensor $\overline{u_i u_j}$ decrease in magnitude when scaled with outer variables (here, the centerline mean velocity of the Poiseuille flow U_c and the channel half-width h) as DR increases. Yet the diminution of the rms u' of the streamwise velocity fluctuations is small compared to v', w' or $\overline{uv}$ and it results in an increase of the maximum of u'^+ in the wall region ($^+$ denotes the scaling by inner variables based on the skin-friction velocity u_τ and the viscosity ν). LDR produces the largest maximum values of u'^+ whereas the peak seems to reduce back to the $DR = 0\%$ case at HDR and MDR. The latter regime is still not completely understood from a physical point of view and will not be further discussed here.

1.2. *Conceptual model for the mechanism of polymer drag reduction*

Using Brownian dynamics simulation, Terrapon *et al.* (2004) showed that polymers experience significant stretching in upwash and downwash flows generated by vortices. Dubief *et al.* (2004) completed Terrapon's work by studying how polymers interact with coherent structures. The viscoelastic simulations performed in this latter article confirmed that polymers extract energy from vortices causing them to weaken. In the meantime, a significant part of the energy stored by polymers that are caught in downwash flows is released in high-speed streaks where viscous forces dominate. The damping of streamwise velocity fluctuations by Newtonian forces is therefore countered by viscoelastic forces. Dubief *et al.* (2004) then proceeded to incorporate polymers in the regeneration cycle of near-wall turbulence as proposed by Jiménez & Pinelli (1999), as sketched in Fig. 1. For

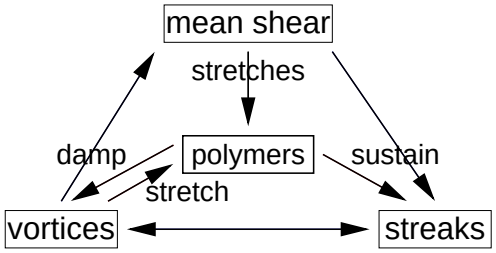

FIGURE 1. Model of the mechanism of polymer drag reduction in near-wall turbulence.

a Newtonian flow, the mean shear gives birth to streaks through instabilities. Perturbations and instabilities then produce vortices which transfer momentum vertically and sustains the mean shear. According to the dynamics introduced earlier, polymers sits at the center of this regeneration cycle as shown in Fig. 1.

2. Governing equations and numerical method

2.1. *Polymer model*

The evolution of polymers is represented on the basis of bead-spring (dumbbell) models. Each dumbbell is subject to the hydrodynamic forces exerted by the flow on the beads, the spring force and Brownian forces. The balance of forces gives an evolution equation for the end to end dumbbell vector $\mathbf{q}$, known as the FENE model (Finitely Extensible Nonlinear Elastic). A constitutive approach is obtained by taking into account the Brownian motion using a phase average of the product of the $\mathbf{q}$-components, which defines the conformation tensor $c_{ij} = \langle q_i q_j \rangle$. The hydrodynamic and relaxation (spring) forces are explicitly simulated; the latter force can be estimated with various models. The model used here is the FENE-P model, where P stands for the Peterlin function, f, defining the following set of equations

$$\partial_t c_{ij} + u_k \partial_k c_{ij} = c_{kj}\partial_k u_i + c_{ik}\partial_k u_j - \frac{1}{\lambda}(f c_{ij} - \delta_{ij}) \ , \tag{2.1}$$

$$f = \frac{1}{1 - c_{kk}/L^2} \, . \tag{2.2}$$

The parameter L is the maximum polymer extension and λ is the relaxation time of the polymers. The relevant non-dimensional quantity to describe a polymer solution is the Weissenberg number, We, the ratio of the polymer to the flow time scales which can be the outer or inner scales:

$$We = \frac{\lambda U_c}{h} \text{ or } We_\tau = \frac{\lambda u_\tau^2}{\nu} \ , \tag{2.3}$$

where u_τ is the skin-friction velocity of the Newtonian flow, unless specified otherwise. U_c and h are the integral scales for a channel flow, namely the centerline velocity and the channel half-width. Finally the contribution of polymers to the flow is brought in the momentum equations via the divergence of the polymeric stress tensor τ_{ij},

$$\tau_{ij} = \frac{1}{\lambda}(f c_{ij} - \delta_{ij}) \ , \tag{2.4}$$

run	$We_{\tau 0}$	β	b
1	36	0.9	10000
2	60	0.9	3600
3	120	0.9	10000
4	36	0.9	19600
5	36	0.9	3600
6	60	0.9	19600
7	40	0.4	25600

TABLE 1. Polymer parameters for the channel flow DNS database used for the validation of $v^2 - f - p$. The Reynolds number

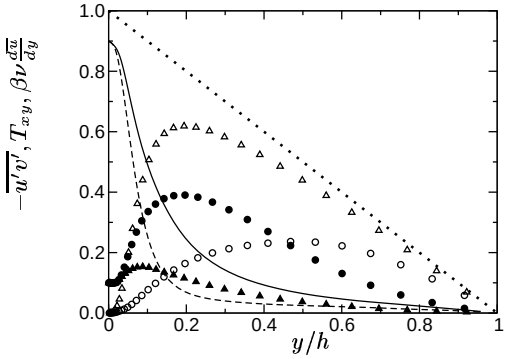

FIGURE 2. Contributions of the Reynolds shear, polymer and viscous stresses to the balance Eq. (2.6. For LDR: ——— , $\beta\nu\frac{d\overline{u}}{dy}$; ∘ , $-\overline{u'v'}$; • , T_{xy}. FOR HDR: – – – – , $\beta\nu\frac{d\overline{u}}{dy}$; △ , $-\overline{u'v'}$; ▲ , T_{xy}. ····· , $1 - \frac{y}{h}$. The stresses are normalized by u_τ and ν.

yielding the viscoelastic momentum equations,

$$\partial_t u_i + u_j \partial_j u_i = -\partial_i p + \beta\nu\partial_j\partial_j u_i + (1-\beta)\nu\partial_j \tau_{ij} \ , \tag{2.5}$$

where β is the ratio of the solvent viscosity ν_s to the total viscosity ν. The last term in the rhs of Eq. (2.5) is the contribution of the viscoelastic stress to the flow.

2.2. *Reference DNS solutions*

The model development and validation is performed using a series of DNS solutions in a channel flow. The numerical method for the DNS calculations is described in Dubief *et al.* (2005).

The Reynolds number based on the bulk velocity is $Re_M = 5000$, $Re_\tau = 300$ based on the skin-friction velocity. The flow is driven by conservation of the mass flow. The runs used for the present study are summarized in Table 1.

2.3. *Statistical properties of LDR and HDR*

A RANS model is based on statistical equations derived from the momentum equations (Eq. 2.5). In the case of interest here, the balance of stresses is:

$$-\overline{u'v'} + \beta\nu\frac{d\overline{u}}{dy} + T_{xy} = \left[-\frac{d\overline{p}}{dx}\right]\left(1 - \frac{y}{h}\right) \ , \tag{2.6}$$

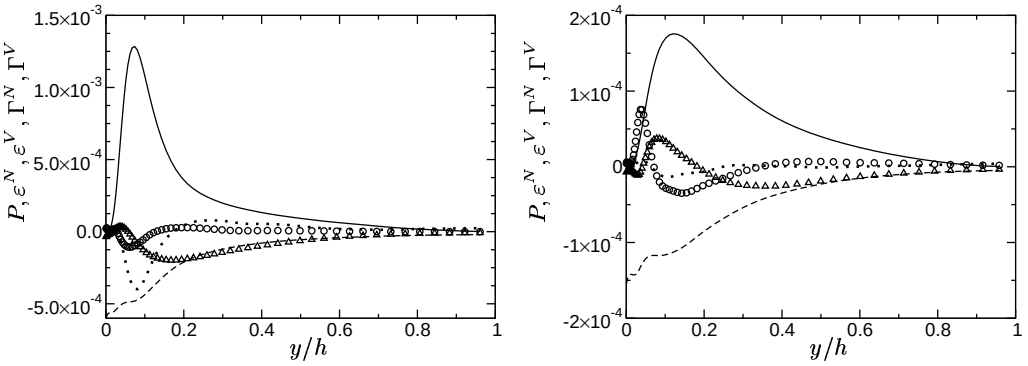

FIGURE 3. Production, Newtonian and viscoelastic dissipation, Newtonian and viscoelastic transport terms for LDR (*left*) and HDR (*right*). (runs 1 and 3 of Tab. 1, respectively). ——— , P; ····· , Γ^N; – – – – , ε^N; □ , ε^V; ○ , Γ^V;

where T_{xy} is the polymer stress

$$T_{xy} = (1-\beta)\nu \frac{d\overline{\tau}_{xy}}{dy} \tag{2.7}$$

Hereafter, the instantaneous quantities are decomposed in a mean and fluctuating part, $u = \overline{u} + u'$. The Reynolds shear stress, viscous stress and polymer stress are plotted in Fig. 2 for LDR (DR=30%, run 1) and HDR (DR=60%, run 3). The polymer stress increases with increasing DR to become comparable to (or larger than) the Reynolds shear stress at HDR.

The second equation to be modeled is usually the turbulent kinetic energy budget,

$$\begin{aligned}\partial_t \overline{u_i' u_j'} + \overline{u}_k \partial_k \overline{u_i' u_j'} = & \underbrace{-\overline{u_i' u_k'} \partial_k \overline{u}_j - \overline{u_j' u_k'} \partial_k \overline{u}_i}_{P} \underbrace{-\partial_k \overline{u_i' u_j' u_k'}}_{\Gamma^N} \\ & - \left(\overline{u_i' \partial_j p' + u_j' \partial_i p'}\right) + \beta\nu \partial_k \partial_k \overline{u_i' u_j'} - \underbrace{2\beta\nu \overline{\partial_k u_i' \partial_k u_j'}}_{\varepsilon^N} \\ & \underbrace{+(1-\beta)\nu \partial_k \left(\overline{u_i' \tau_{jk}' + u_j' \tau_{ik}'}\right)}_{\Gamma^V} \underbrace{- (1-\beta)\nu \overline{\tau_{ik} \partial_k u_j' + \tau_{jk}' \partial_k u_i'}}_{\varepsilon^V}\end{aligned} \tag{2.8}$$

Even though, the $v^2 - f$ model incorporates closures for all the Newtonian terms, it is of interest to get an indication of the behavior of production (P), dissipation (ε) and turbulent transport (Γ), relative to the additional viscoelastic terms as shown in Fig. 3. The superscripts N and V denote Newtonian and viscoelastic dissipation and transport, respectively. For clarity, the velocity pressure gradient term and the diffusion term are not plotted. The role of polymers is observed to increase relatively to the production and Newtonian dissipation as DR increases. The near-wall behavior is further discussed in the modeling section.

2.4. $v^2 - f$ model

The model used for polymer drag reduction is the $v^2 - f$ model developed by Durbin (1995). This model is an extension of the classical $k - \varepsilon$ model to correctly represent the near-wall behavior (and viscous damping) of the turbulent quantities. This is realized by a modification of the eddy-viscosity formulation and by solving two additional partial

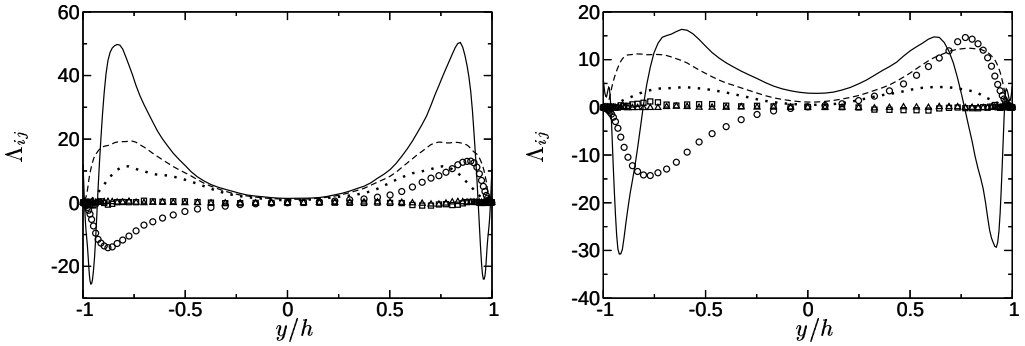

FIGURE 4. Components of the stretching tensor Λ_{ij} for LDR (*left*) and HDR (*right*). (runs 1 and 3 of Tab. 1, respectively). ——— , Λ_{11}; ····· , Λ_{22}; – – – – , Λ_{33}; ∘ , Λ_{12}; □ , Λ_{13}; △ , Λ_{23}.

differential equations: a transport equation for the turbulent intensity of the velocity fluctuations $\overline{v'^2}$ normal to the streamlines and an elliptic relaxation equation for f. The latter represents the effect of the turbulence redistribution. The major advantage of $v^2 - f$ over $k - \varepsilon$ is the absence of wall-damping function. The model solves the following equations:

- turbulent viscosity

$$\nu_t = 0.22\overline{v'^2}T_t \tag{2.9}$$

- kinetic energy transport equation

$$\partial_t k_t + \overline{u}_i \partial_i k_t = P_t - \varepsilon + \partial_j \left[(\nu + \nu_t)\, \partial_j k_t\right] \tag{2.10}$$

- dissipation transport equation

$$\partial_t \varepsilon + \overline{u}_j \partial_j \varepsilon = \partial_j \left(\frac{\nu_t}{1.3}\partial_j \varepsilon\right) + \frac{1}{T_t}\left(-1.4\sqrt{1 + 0.045k/\overline{v'^2}}P_t - 1.9\varepsilon\right) \tag{2.11}$$

- v^2 transport equation

$$\partial_t \overline{v'^2} + \overline{u}_j \partial_j \overline{v'^2} = k_t f - 6\overline{v'^2}\frac{\varepsilon}{k} + \partial_j \left[(\nu + \nu_t)\, \partial_j \overline{v'^2}\right] \tag{2.12}$$

- elliptic relaxation equation for f

$$f - L_t^2 \partial_j \partial_j f = 1.4\frac{2/3 - \overline{v'^2}/k_t}{T_t} + 0.3\frac{P_t}{k_t} + \frac{5\overline{v'^2}/k}{T_t} \tag{2.13}$$

- turbulent production (S is the mean strain rate tensor, $S_{ij} = (\partial_j \overline{u}_i + \partial_i \overline{u}_j)$)

$$P_t = \nu_t S^2 \tag{2.14}$$

- turbulent length and time scales

$$T_t = \max\left[\frac{k_t}{\varepsilon}, 6\left(\frac{\nu}{\varepsilon}\right)^{1/2}\right], \; L_t = 0.3\max\left[\frac{k_t^{3/2}}{\varepsilon}, 70\left(\frac{\nu^3}{\varepsilon}\right)^{1/4}\right] \tag{2.15}$$

3. $v^2 - f - p$ model

3.1. *Modeling the polymer dynamics in turbulent flows*

The tensorial nature of the FENE-P model makes it complex and unattractive in the context of a simple eddy-viscosity based closure. The modeling of the stretching term is non-trivial as shown by Fig. 4 where the individual components of the tensor

$$\Lambda_{ij} = \overline{c'_{ik}\partial_k u'_j} + \overline{c'_{kj}\partial_k u'_i} \,. \tag{3.1}$$

Of particular importance is the modeling of the near-wall behavior of Λ_{xx}. The negative peak marks the region where polymers inject energy into turbulence, which explains why this phenomenon is more pronounced at HDR. Note that Λ_{kk} and the viscoelastic dissipation (3) have similar behavior, yet opposite in sign. Using the quantities available from v^2-f, k_t, $\overline{u}_i$, $\overline{u'_i u'_j}$ and S_{ij}, did not yield satisfactory models. This approach required individual constants per components and failed to reproduce the near-wall behavior so important to the transfer of energy from the polymers to turbulence.

The difficulty of modeling Λ_{ij} has motivated the development of an algrebaic model capable of capturing the energy transfer between polymers and turbulence. Instead of focusing on the stretching term alone, a simpler measure of this energy exchange is considered: the polymer elongation, c_{ii}. When turbulence stretches polymers, turbulent energy is stored by the polymers. When polymers coil, elastic energy is released in turbulence. Fig. 5 outlines the difference between LDR and HDR in terms of the distribution of c_{ii} in the near wall region where local extrema can be interpreted as relative stretching (local maximum) or recoil (local minimum). The dip close to the wall defines therefore the region where elastic energy goes to streaks (see the model of polymer drag reduction, Fig. 1). Further away from the wall, the local maximum located in the buffer region denotes the vortex damping action of the polymers.

The evolution equation for polymer elongation can be recast as

$$D_t c_{ii} = \underbrace{2c_{ij}\partial_j u_i}_{\text{production}} \underbrace{- \frac{1}{\lambda}\left(f c_{ii} - 3\right)}_{\text{destruction}} , \tag{3.2}$$

where $D_t = \partial_t + u_j\partial_j$. The stretching term is analogous to a production term, while the relaxation term effectively destroys elongation. In this framework familiar to RANS modeling, we can develop models based on our physical understanding of the phenomenon. Note that Eq. (3.2) is unclosed due to the cross terms present in the production term. The modeling is developed here only for steady-state channel flow with homogeneous concentration of polymers for which the transport terms in $\overline{D_t c_{ii}}$ vanish. In the destruction term, the first order approximation $\overline{f c_{ii}} = \overline{f}\,\overline{c}_{ii}$ is reasonable as shown in Fig. 5 and will be used in the following. Using our conceptual model of the mechanism of polymer drag reduction (Fig. 1), we decompose the production into two contributions: contribution from the mean shear and contribution from turbulence, which, in our schematic representation in Fig. 1, would be the vortices.

If the polymers were subject to the mean shear only, the FENE-P model would reduce to:

$$\overline{c}_{ik}\partial_k\overline{u}_j + \overline{c}_{kj}\partial_k\overline{u}_i - \frac{1}{\lambda}\left(\overline{f}\,\overline{c}_{ij} - \delta_{ij}\right) = 0 \,. \tag{3.3}$$

For the steady-state channel flow, the system reduces to a single equation, third-order

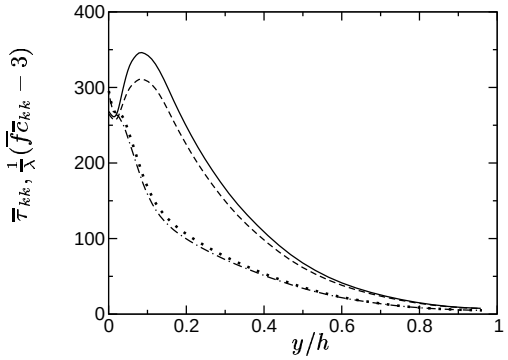

FIGURE 5. Approximation of $\overline{\tau}_{kk}$ by $\frac{1}{\lambda}(\overline{f}\overline{c}_{kk} - 3)$of for LDR and HDR . (runs 1 and 3 of Tab. 1, respectively). ——— : exact, HDR; ····· : exact, LDR; - - - - : approximation, HDR; —·— : approximation, LDR.

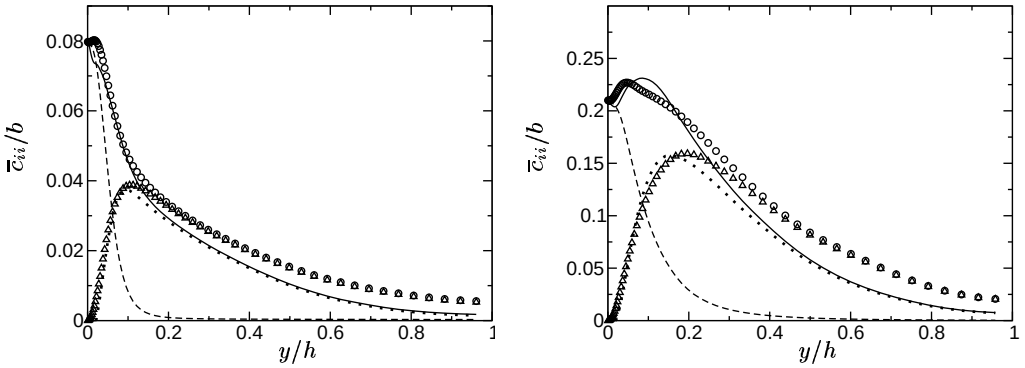

FIGURE 6. Modeling of the mean polymer extension $\overline{c}_{ii}$ for LDR (*left*) and HDR (*right*). (runs 1 and 3 of Tab. 1, respectively). ——— , exact $\overline{c}_{ii}$; - - - - , $\overline{c}_{ii}^M$ obtained from the mean shear only (Eq. 3.4); ····· , $\overline{c}_{ii} - \overline{c}_{ii}^M$; $\triangle$, model for $\overline{c}_{ii} - \overline{c}_{ii}^M$; $\circ$, model for $\overline{c}_{ii} - \overline{c}_{ii}^M$.

polynomial in $\overline{f}$:

$$0 = 2\frac{\lambda S^2}{\overline{f}^2} - \frac{1}{\lambda}\left(\overline{f}\,\overline{c}_{kk} - 3\right) \ , \tag{3.4}$$

where S^2 reduces to $(\partial_y \overline{u})^2$. The solution of this polynomial is shown in Fig. 6 for LDR and MDR regimes. The wall value of $\overline{c}_{kk}$ is accurately predicted by Eq. (3.4) since turbulent velocity fluctuations vanish at the wall, leaving the mean shear as the only stretching source for the polymers.

The turbulent contribution to stretching, difference between the total elongation and the solution to Eq. (3.4), is very similar to the profile of kinetic energy across the channel flow, as shown in Fig. 6. This resemblance has prompted a model based around $k_t\lambda$ which can be interpreted as a *turbulent viscoelastic viscosity*, ν_{tp}. The effect of turbulence on polymers is so far described as a linear function of the polymer length b. The proper scaling of this model imposes the introduction of a turbulent length scale h. The choice for this length scale is still not clear and in the following, h is chosen as the channel half-width. Polymers can only be stretched by turbulent eddies only if the time scales of the eddies is larger than the relaxation time scale. Therefore, under the approximations considered for the present study, the trace of the conformation tensor is governed by the

following equation:

$$0 = 2\frac{\lambda S^2}{\overline{f}^2} + \gamma_1 b \frac{k_t \lambda}{h^2} - \frac{1}{\lambda}\left(\overline{f}\overline{c}_{kk} - 3\right) \ . \tag{3.5}$$

3.2. *Modeling the effect of polymers on turbulent structures*

In the recent extensive statistical studies performed using viscoelastic DNS, it was observed that most turbulent quantities decrease with increasing drag reduction (see Dimitropoulos *et al.* 2001, for instance). From a RANS viewpoint, the pressure-strain term decrease needs to be accurately modeled since it determines the level of anisotropy of the flow and has a direct effect on the behavior the mean velocity, especially in the log-region. Our first attempt was to add a term in the elliptic equation (2.13) which is the effective pressure redistribution mechanism in the $v^2 - f$ model. This addition was inspired by Leighton *et al.* (2003) who developed a Reynolds-stress model for LDR flows. We found the term to be able to reproduce the upward shift in the log-law but the solution is extremely sensitive to the user-defined constant related to this term. By increasing the constant, the flow becomes laminar without ever showing any HDR characteristics.

It was then suggested to us (P. Durbin, private communication) that Eq. (2.13) is controlled by the turbulent length scale $L_t = C_L k_t^{3/2}/\varepsilon$. We can then argue that the drop in pressure-strain is a mere consequence of the increase of the typical length scale of turbulent structures (vortices and streaks), which translates into an augmentation of L_t. This increase must be a function of the polymer concentration, β in the case of the FENE-P model, the relaxation time λ or We and the local polymer stretching. We propose a linear dependence on these quantities as a first approximation yielding

$$L_t = C_L \left(1 + \gamma_L (1-\beta)\frac{c_{ii}}{b} We\right) \frac{k_t^{3/2}}{\varepsilon} \tag{3.6}$$

where We is used instead of λ to satisfy the non-dimensionality of the viscoelastic function.

The modeling of the interaction between polymers and turbulence uses an approach similar to the one developed for the polymer dynamics. In the balance of stresses, the viscoelastic stress $\overline{T}_{xy} = (1-\beta)\overline{\tau}_{xy}$ is decomposed in its solution for the mean shear and a model for the contribution of turbulence. The viscoelastic stress can then be written in a Boussinesq-like form:

$$\overline{T}_{ij} = (1-\beta)\left(\frac{\nu}{\overline{f}} + \underbrace{\gamma_\nu k_t \lambda}_{\nu_{tp}}\right) S_{ij} \tag{3.7}$$

The viscoelastic contribution to the kinetic energy equation is then modeled using the turbulent viscoelastic viscosity in the form of a production term:

$$\partial_t k_t + \overline{u}_i \partial_i k_t = P_t + P_{tp} - \varepsilon + \partial_j \left[\left(\nu + \nu_t\right)\partial_j k_t\right] \tag{3.8}$$

with

$$P_{tp} = \nu_{tp} S^2 \ . \tag{3.9}$$

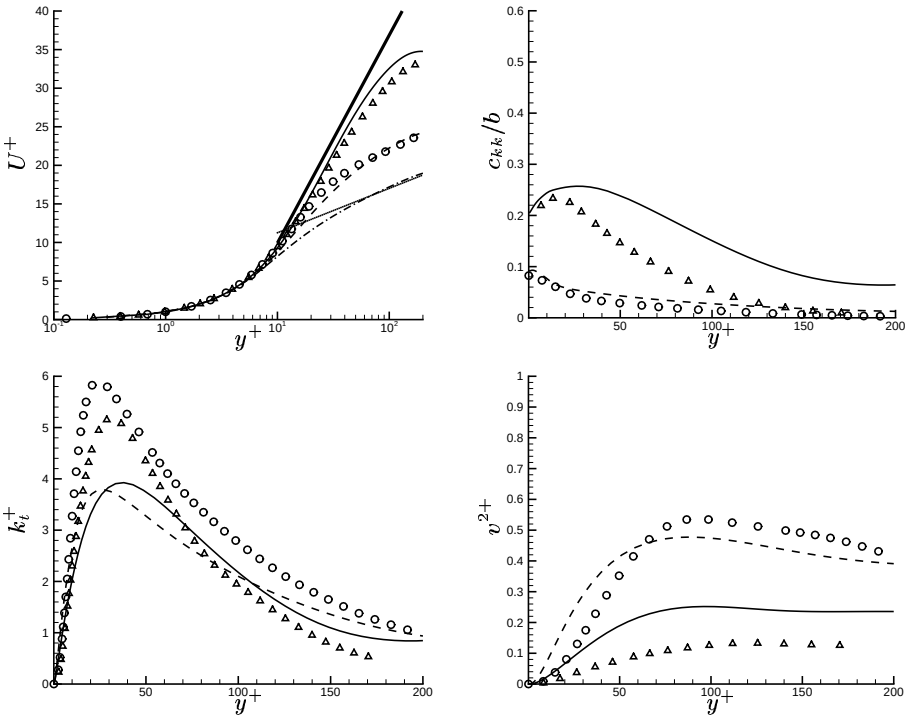

FIGURE 7. Comparison between $v^2 - f - p$ and DNS for $Re_M = 5000$, $b = 10000$ at LDR ($We_\tau = 36$: $\circ$, DNS; - - - - , $v^2 - f - p$) and HDR ($We_\tau = 120$: $\triangle$, DNS; ——— , $v^2 - f - p$) 0*Upper left*: mean velocity profiles. —·— , $v^2 - f - p$ (Newtonian flow); ····· , Newtonian log-law ($U^+ = 2.5\ln(y^+) + 4.1$); ——— , Virk's asymptote ($U^+ = 11.7\ln(y^+) - 17$). *Upper right*: Polymer elongation . *Lower left*: Turbulent kinetic energy. *Lower right* Wall-normal velocity fluctuations.

4. Channel flow predictions

The calibration and validation of our model is based on our database of viscoelastic DNS runs performed in a channel flow at $Re_M = 5000$, described in Table 1. These runs cover most of the physical parameters for realistic polymer simulations. The three constants entering the model $v^2 - f - p$ are adjusted using run 1 (LDR, DR=35%) and 3 (HDR, DR=60%) only. The mean velocity profiles for these two runs (Fig. 7) are found to exhibit the expected behavior, namely a shift of the log-law for LDR and the right change of slope for HDR. The mean polymer elongation is overestimated, however, $v^2 - f - p$ captures the maximum away from the wall, critical feature of HDR. The kinetic energy and wall-normal velocity fluctuations are also overpredicted, nevertheless they are shown to decrease with increasing DR. Finally the comparison for the calibration runs and the remaining runs is depicted in Fig. 8. The agreement is very good with DR (%) predicted with a $\pm 5\%$ accuracy.

5. Conclusion and future work

The prediction of drag-reduced turbulent polymer flows has been shown to be within reach using the $v^2 - f$ model. The current model $v^2 - f - p$ is simple and robust:

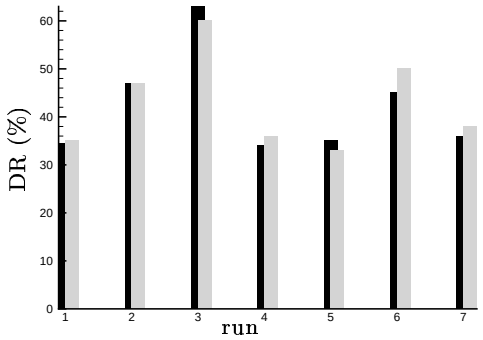

FIGURE 8. Comparison between $v^2 - f - p$ (dark bars) and DNS for $Re_M = 5000$ for various relaxtion time and polymer length described in Tab. 1

only three additional constants and no ad-hoc wall functions are introduced. It proves to accurately reproduce drag reductions computed from channel flow direct numerical simulations. More importantly, the model predicts the right change of slope of the mean velocity profile in the log-law region, for the first time without any direct assumption on the slope change in the tuning of the coefficients.

The model is nevertheless at its very early stage. Although the results are extermely encouraging, the closure for the production term of the polymer elongation transport equation (Eq. 3.5) is not satisfactory, since it involves one arbitrary length scale and there is no dependence on a turbulent time scale. The linearity in the closure for the turbulent length scale also needs to to be investigated especially toward MDR. The future work will include the development of a closure for the transport term for $\overline{c}_{ii}$ and the addition of the transport equation for the polymer concentration in order to simulate turbulent boundary layers subject to injection of polymers from a slot.

The support of DARPA and its project manager, Dr. Lisa Porter, are gratefully acknowledged. This work is sponsored by Defense Advanced Research Projects Agency, Advanced Technology Office, Friction Drag Reduction Program, DARPA order No.: K042/31, K042/13,N115/00. Issued by DARPA/CMO, Contract No.: MDA972-01-C-0041.

REFERENCES

DIMITROPOULOS, C. D., SURESHKUMAR, R., BERIS, A. N. & HANDLER, R. A. 2001 Budget of reynolds stress, kinetic energy and streamwise enstrohpy in viscoelastic turbulent channel flow. *Phys. Fluids* **13** (4), 1016–1027.

DUBIEF, Y., TERRAPON, V. E., WHITE, C. M., SHAQFEH, E. S. G., MOIN, P. & LELE, S. K. 2005 New answers on the interaction between polymers and vortices in in turbulent flows. *Flow, Turbulence and Combustion* To appear.

DUBIEF, Y., WHITE, C. M., TERRAPON, V. E., SHAQFEH, E. S. G., MOIN, P. & LELE, S. K. 2004 On the coherent drag-reducing and turbulence-enhancing behavior of polymers in wall flows. *J. Fluid Mech.* **514**, 271–280.

DURBIN, P. A. 1995 Separated flow computations with the $k - \varepsilon - v^2$ model. *AIAA J.* **33**, 659–664.

JIMÉNEZ, J. & PINELLI, A. 1999 The autonomous cycle of near-wall turbulence. *J. Fluid Mech.* **389**, 335–359.

LEIGHTON, R. I., WALKER, D. T., STEPHENS, T. R. & GARWOOD, G. C. 2003 Reynolds-stress modeling for drag-reducing viscoelastic flow. In *2003 Joint ASME/JSME Fluids Engineeing Symposium on Friction Drag Reduction*. Honolulu, Hawaii, USA.

MIN, T., YOO, J. Y. & CHOI, H. 2001 Effect of spatial discretization schemes on numerical solutions of viscoelastic fluid flows. *J. Non-Newtonian Fluid Mech.* **100**, 27–47.

TERRAPON, V. E., DUBIEF, Y., MOIN, P., SHAQFEH, E. S. G. & LELE, S. K. 2004 Simulated polymer stretch in a turbulent flow using brownian dynamics. *J. Fluid Mech.* **504**, 61–71.

VIRK, P. S. & MICKLEY, H. S. 1970 The ultimate asymptote and mean flow structures in Tom's phenomenon. *Trans. ASME E: J. Appl. Mech.* **37**, 488–493.

WARHOLIC, M. D., MASSAH, H. & HANRATTY, T. J. 1999 Influence of drag-reducing polymers on turbulence: effects of Reynolds number, concentration and mixing. *Exp. Fluids* **27**, 461–472.